Supplemental Material for:

Small Crowders Slow Down Kinesin-1 Stepping by Hindering Motor Domain Diffusion

Krzysztof Sozański,[1] Felix Ruhnow,[2] Agnieszka Wiśniewska,[1]
Marcin Tabaka,[1] Stefan Diez,[2,*] and Robert Hołyst[1,†]

[1] *Institute of Physical Chemistry, Polish Academy of Sciences, Kasprzaka 44/52, 01-224 Warsaw, Poland*

[2] *B CUBE-Center for Molecular Bioengineering, Technische Universität Dresden, Arnoldstrasse 18, 01307 Dresden, Germany*

(Dated: September 7, 2015)

DETAILS ON MATERIALS AND METHODS

Crowders Used

Designation	M_{W} [kg/mol]	PDI	R_{h} [nm]
PEG 6 kg/mol	6.55	1.06	2.17
PEG 18 kg/mol	17.90	1.20	3.85
PEG 1000 kg/mol	941.0	1.07	65.3
TetraEG	0.194	–	0.3
sucrose	0.342	–	0.5
BSA	66.0	–	3.9
Dextran 10 kg/mol	∼10	–	∼ 2.36
Dextran 500 kg/mol	∼500	–	∼ 14.7

TABLE S1. Crowding agents used throughout the experiments. PDI denotes polydispersity index, calculated as ratio of weight and number average molecular masses of a polymer. Hydrodynamic radii of the PEGs were calculated according to a model described elsewhere [1], R_{h} of BSA was taken from [2], while for TetraEG and sucrose it was directly estimated on the basis of the molecular structure. Data for dextrans supplied by the manufacturer and from [4].

PEGs of molecular weight standard quality were obtained from Polymer Standards Service, GmbH, Mainz, Germany; TetraEG, sucrose, and lyophilized BSA were purchased from Sigma-Aldrich. Dextrans T10 and T500 (approx. M_{W} of 10 and 500 kg/mol, respectively) were obtained from Pharmacosmos (Denmark). Dextrans were not M_{W}-standards and presented a broad distribution of molecular weights.

None of the above crowders revealed specific interactions with the MTs. PEGs are frequently used in vivo as bio-compatible, inert polymers. In a series of imaging and FCS experiments with dextrans injected into HeLa cells (data not shown), we observed mostly free diffusion and no attachment to the MT scaffolding. BSA is used as a negative control in MT affinity assays.

We also performed experiments with lysozyme ($R_{\mathrm{h}} = 1.9$ nm) as crowder. However, it appeared to exhibit strong interactions with the MTs, even at a relatively low concentration

(2.5%). This could be expected since lysozyme has a strong positive charge at neutral pH and is electrostatically attracted to the MTs. Binding and rapid unbinding of kinesin-1 was observed in assays with lysozyme, however no movement events (over observable distances, i.e. at least 300 nm) were recorded. We hypothesize that lysozyme acted as densely located roadblocks. This was qualitatively different from what we observed for other crowders (gradual decrease of velocity and frequency of walking events, long times of kinesin residence in the vicinity of the MT due to depletion effect).

Viscosity Scaling Parameters

System		a	b	Referene / comments
PEGs	entangled	0.78	1.55	[3]
	non-entangled	1.29		
Dextrans	entangled	0.78	2.4 for T10, 3.3 for T500	a as for flexible polymers; b fitted on the basis of data from [4]. Due to the polydyspersity of dextrans and their badly defined length-scales, the values of b are empirically matched for each polymer individually, while final η_{eff} values should be treated as rough estimates
	non-entangled	1.29		
BSA		1.29	22.9	[5]– model for colloidal particles
TetraEG, sucrose		–	–	$r_{\text{p}} \gg R_{\text{h}}$ – macroscopic viscosity (measured by rheometry) equal to η_{eff}

TABLE S2. Viscosity scaling parameters used in Equation 1 (main text) to calculate the effective viscosity experienced by the kinesin-1 motor domain in different solutions.

Motility Assays

The stepping assay using for TIRF microscopy has been extensively described by Korten *et al* [6]. Briefly, we performed the experiments in flow channels [7], self-built from two glass coverslips (22x22 mm and 18x18 mm; Corning, Inc., Corning, NY), which were cleaned

in piranha solution (H_2O_2/H_2SO_4, 3:5; both purchased from Sigma), silanized with 0.05% dichlorodimethylsilane in trichloroethylene (Sigma) and glued together by heated pieces of Parafilm M (Pechiney Plastic Packaging, Chicago, IL). The flow sequence was as follows:

1. The flow cell was filled with a solution of TetraSpeck microspheres (diameter 100 nm; Invitrogen) diluted 200-fold in BRB80 buffer;

2. After 2 min, the solution was exchanged with a BRB80 solution containing 77.5μg/ml anti-β-tubulin antibodies (SAP4G5; Sigma);

3. After 5 min, the surface was blocked with a 1% solution of Pluronic F-127 (Sigma) in BRB80;

4. Taxol-stabilized microtubules [6], diluted ninefold to prevent crossing microtubules, were incubated for 5 min to bind to the tubulin antibodies;

5. Microtubule solution was finally replaced by the motility solution (BRB80 containing 10 μM taxol, 0.04 mM glucose, 0.2 mg/ml glucose oxidase, 0.02 mg/ml catalase, 10 mM DTT, 0.1 mg/ml casein, 1mM Mg-ATP, 0.1% Tween 20; all from Sigma) supplemented by 4 μg/ml of truncated, GFP-labeled kinesin-1 (rKin430-6HIS-GFP) [8] and additional molecular crowding agents.

Optical Imaging

Fluorescence imaging was performed using an inverted fluorescence microscope (Zeiss Observer Z1; Zeiss, Jena, Germany) with a 100x oil immersion objective (Zeiss APOCHROMAT ; numerical aperture 1.46; Zeiss) with an additional 1.33x magnifying optovar. The final pixel size was 117 nm. Microtubules were observed by epifluorescence using a Lumen 200 metal arc lamp (Prior Scientific Instruments Ltd., Fulbourn, UK) with a TRITC (exc 534/30, em 593/40, dc R561; all Chroma Technology, Rockingham, VT) filter set. Kin430-GFP motor proteins were observed in total internal reflection fluorescence (TIRF) mode, by using a PhoxX 488 nm Laser (Omicron-Laserage, Rodgau-Dudenhofen, Germany) with a GFP (exc 470/40, em 525/50, dc 495; all Zeiss) filter set. Image acquisition was performed at 100 ms exposure time in streaming mode by an electron-multiplied charge-coupled device camera (iXon Ultra DU-897U; Andor, Belfast, Northern Ireland) in conjunction with

a Metamorph imaging system (Universal Imaging Corp., Downingtown, PA). On the basis of stacks of 1500 subsequently recorded images, kymographs were constructed using FIESTA software [9]. From such 2D representation of motion (position of the labeled kinesin molecule along the MT vs. time) velocity of each individual motor was read. Only linear movement was included, disregarding any stall or stop-and-go events. Velocities of at least 200 molecules were measured for each stack; three to five stacks were recorded for each assay. In experiments where zero velocity is reported, no traces covering at least 3 pixels (corresponding to a molecule displacement of at least 350 nm) were observed. Errors are reported as standard deviation of the mean for all the molecules observed in a given assay.

Fluorescence Correlation Spectroscopy and Rheometry

Fluorescence correlation spectroscopy (FCS) measurements were performed using a Nikon C1 inverted confocal microscope equipped with a full TCSPC system from PicoQuant GmbH, Berlin, Germany. The instrument featured a 488 nm diode laser, 60x WI Nikon Plan Apo objective and two single-photon counting devices working in parallel. Temperature of the sample was kept at 298.0±0.5 K throughout all the experiments. The probe was the same construct as used in the motility assays, i.e. rKin430-6HIS-GFP. No significant bleaching issues were observed. Fluorescence intensity time traces revealed no sudden bursts, which would indicate the presence of fluorescent aggregates. At least 10 independent autocorrelation curves were recorded for each sample within the SymPhoTime software package. Global fitting to a one-component free diffusion model was performed using Gnuplot software.

Macroscopic viscosity measurements were performed using a Malvern Kinexus Pro rotational rheometer. A cone-plate geometry was applied throughout all the measurements. As the goal of the measurements was to establish the viscosity at zero shear rate, which was not directly possible, measurements were performed with precise control of the shear stress in the range of 0.01 to 10 Pa and then linear extrapolation was performed. Sample temperature was kept at 298.0±0.1 K.

SUPPORTING FIGURES

Viscosity Scaling Plots

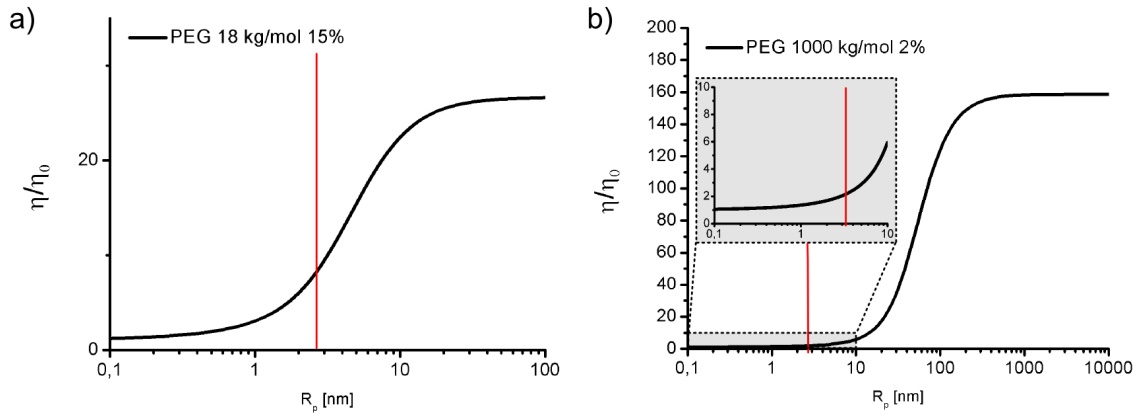

FIG. S1. Viscosity scaling according to Eq. 1 (main text) [10]. The effective viscosity η of a complex liquid experienced by a probe is a function of the hydrodynamic radius of the probe, r_{p}. Plots **a** and **b** illustrate this dependence for a 15% aqueous solution of 18 kg/mol PEG and a 2% solution of 1000 kg/mol PEG, respectively. η_0 is solvent viscosity. Red line corresponds to estimated r_{p} of a kinesin head. Although the macroscopic viscosity (large probe limit) in case **a** is lower than in case **b** by nearly an order of magnitude, a nanoscopic kinesin head experiences lower viscosity in case **b**.

Fluorescence Correlation Spectroscopy Results

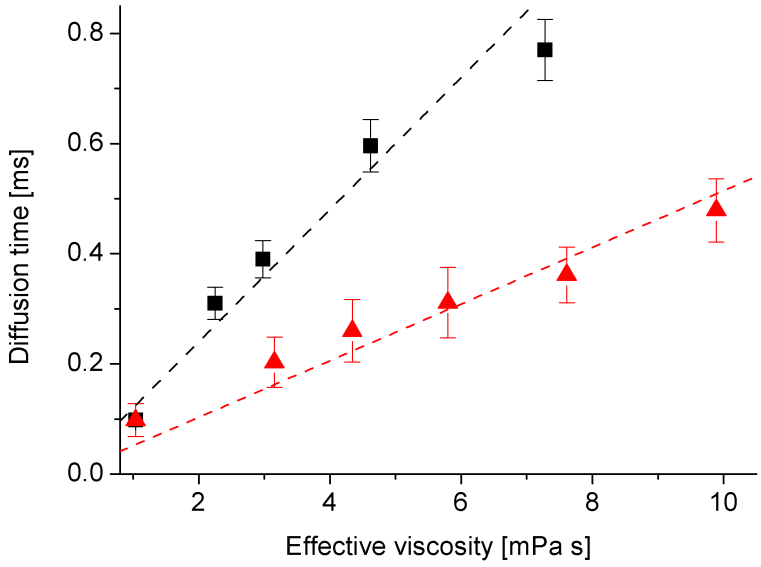

FIG. S2. Diffusion times of rKin430-6HIS-GFP measured by FCS for different concentrations of TetraEG (squares) and 18 kg/mol PEG (triangles). In both cases, the diffusion times depend linearly on the effective viscosity. No aggregation of kinesin is observed, which would cause a rapid, non-linear increase of diffusion time due to a change of the hydrodynamic radius of the probe. The difference in the slopes is mostly due to expansion of the focal volume in TetraEG solutions of high refractive index.

Kinesin motility at low ATP conditions

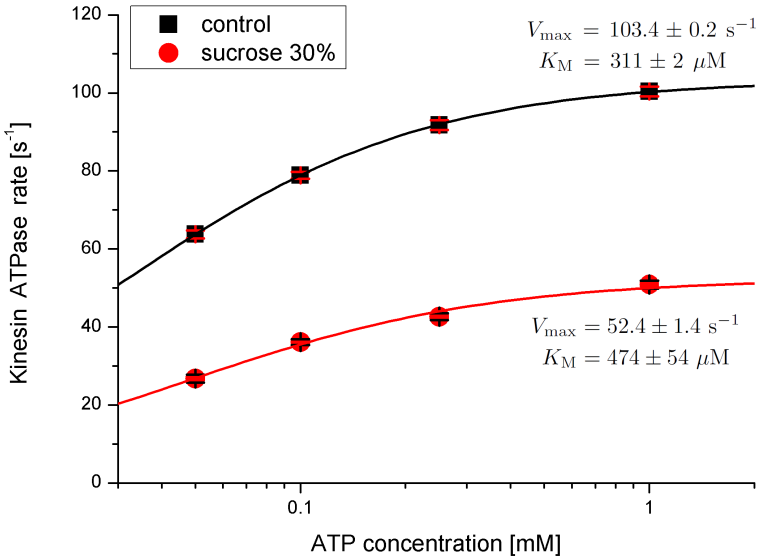

FIG. S3. Kinesin-1 turnover rate, calculated as the quotient of measured stepping velocity and step length of 8 nm, plotted as function of ATP concentration. A solution containing 30% sucrose (i.e. the smallest crowder in this study) is compared with a non-crowded control. Solid lines are fits of the simple Michaelis-Menten kinetic model.

To provide further support for the hypothesis that limited ATP availability is not the cause of kinesin slow-down in crowded environment, we performed a series of experiments at lowered ATP concentration. We compared control assays (no crowders) with 30% sucrose solutions. We used sucrose here as the smallest crowder appearing throughout the study ($R_h \approx 0.5$nm), which therefore should have the highest impact on the diffusion of small ATP molecules ($R_h \approx 0.6$nm).

In Figure S3, simple Michaelis-Menten kinetic model is used to fit the data concerning the kinesin reaction rate: $V = V_{max}[\mathrm{ATP}]/(K_M + [\mathrm{ATP}])$, where V – kinesin turnover rate, V_{max} – maximum reaction rate, K_M – Michaelis constant, [ATP] – ATP concentration. Here, the assumption is made that the stepping rate is directly proportional to the kinesin-1 ATPase rate and that ATP is the sole substrate of the reaction. The model is relevant in both control experiment and sucrose-crowded assay. However, the kinetic parameters K_M and V_{max} change upon introduction of crowding agents. This suggests that the observed

decrease of the stepping velocity is not due to a decrease of the effective ATP concentration, but rather stems from a disturbance in the mechanism of the enzymatic reaction. Such observation is in line with the proposed model of stepping rate limited by the diffusion of the tethered motor domain.

It should also be noted that in the presence of sucrose the diffusion rate of ATP decreases about 3.5 times and the kinesin velocity drops by half. A nearly 20x decrease in ATP concentration in assays with no crowders results in a velocity decrease of 37%. This strongly suggests that ATP availability is not crucial for the velocity decrease in crowded environment. Moreover, an increase of ATP concentration from 1 to 10 mM did not influence the velocity of kinesin in crowded systems (data not shown).

Depletion Interactions – Estimated Osmotic Pressure

Solution	Concentration [% w/w]	Π [kPa]	$\Delta G[k_{\mathrm{B}}T]$
PEG 6 kg/mol	5.0	0.53	1.09
	7.5	1.38	1.84
	10.0	2.63	5.41
	14.0	4.91	10.11
PEG 18 kg/mol	3.0	0.041	0.15
	5.0	0.068	0.25
	10.0	0.14	0.51
PEG 1000 kg/mol	0.25	$6.1 \cdot 10^{-5}$	$2.3 \cdot 10^{-3}$
	0.5	$1.2 \cdot 10^{-4}$	$4.5 \cdot 10^{-3}$
	1.0	$2.5 \cdot 10^{-4}$	$9.0 \cdot 10^{-3}$
	2.0	$4.9 \cdot 10^{-4}$	$1.8 \cdot 10^{-2}$

TABLE S3. Estimation of the influence of osmotic pressure Π on the energy required for detachment of kinesin head from the MT in polymer solutions. Data on Π for 6 kg/mol PEG taken from [11]; for other polymers Π was calculated as for the ideal case – some underestimation is therefore probable. ΔG obtained as volume expansion work performed against pressure Π over a volume corresponding to a cylinder of radius equal to kinesin head hydrodynamic radius (2.5 nm) and height of the polymer coil's diameter.

* Corresponding author: diez@bcube-dresden.de

† Corresponding author: rholyst@ichf.edu.pl

[1] K. Devanand and J. C. Selser, Macromolecules **24**, 5943 (1991).

[2] S. Yadav, S. J. Shire, and D. S. Kalonia, Pharmaceutical research **28**, 1973 (2011).

[3] A. Wiśniewska, K. Sozański, T. Kalwarczyk, K. Kędra-Królik, C. Pieper, S. A. Wieczorek, S. Jakieła, J. Enderlein, and R. Hołyst, Polymer **55**, 4651 (2014).

[4] Y. Rong, *Probing The Structure of Dextran Systems and Their Organization* (Thesis – Graduate School-New Brunswick, Rutgers, New Jersey, 2008).

[5] T. Kalwarczyk, K. Sozanski, S. Jakiela, A. Wisniewska, E. Kalwarczyk, K. Kryszczuk, S. Hou, and R. Holyst, Nanoscale **6**, 10340 (2014).

[6] T. Korten, B. Nitzsche, C. Gell, F. Ruhnow, C. Leduc, and S. Diez, in *Single Molecule Analysis*, Methods in Molecular Biology, Vol. 783, edited by E. J. G. Peterman and G. J. L. Wuite (Humana Press, 2011) pp. 121–137.

[7] C. Gell, V. Bormuth, G. J. Brouhard, D. N. Cohen, S. Diez, C. T. Friel, J. Helenius, B. Nitzsche, H. Petzold, J. Ribbe, E. Schaffer, J. H. Stear, A. Trushko, V. Varga, P. O. Widlund, M. Zanic, and J. Howard, in *Microtubules, in vitro*, Methods in Cell Biology, Vol. 95, edited by L. Wilson and J. J. Correia (Academic Press, 2010) pp. 221 – 245.

[8] K. R. Rogers, S. Weiss, I. Crevel, P. J. Brophy, M. Geeves, and R. Cross, EMBO Journal **20**, 5101 (2001).

[9] F. Ruhnow, D. Zwicker, and S. Diez, Biophys. J. **100**, 2820 (2011).

[10] T. Kalwarczyk, N. Ziębacz, A. Bielejewska, E. Zaboklicka, K. Koynov, J. Szymański, A. Wilk, A. Patkowski, J. Gapiński, H.-J. Butt, and R. Hołyst, Nano Lett. **11**, 2157 (2011).

[11] N. P. Money, Plant Physiol. **91**, 766 (1989).